Gao, N., *et al.*: An Equivalent Temperature Model of 3-D Steady Heat ...
THERMAL SCIENCE: Year 2021, Vol. 25, No. 2A, pp. 1081-1094

1081

AN EQUIVALENT TEMPERATURE MODEL OF 3-D STEADY HEAT CONDUCTION ANALYSIS FOR A FIBER METAL LAMINATED PLATE COATED WITH A THERMAL BARRIER

by

Ninghua GAO[a], Junwei LIAN[b], Zhaohui XU[b], and Haojie JIANG[b]*

[a] School of Science, Zhejiang University of Science and Technology, Hangzhou, China
[b] College of Mechanical Engineering, Zhejiang University of Technology, Hangzhou, China

In this paper, an equivalent temperature model of 3-D steady heat conduction analysis for a fiber metal laminated plate coated with a thermal barrier is presented. The separate variable method and equivalent temperature method are applied comprehensively to solve the temperature field at the interface between the thermal barrier and top aluminum 2024-T3 layer for the fiber metal laminated structure firstly, and values of other layers' temperature and thermal contact resistance are obtained based on balance principle of heat flux between respective adjacent top and bottom layers subsequently. The aim of this research is to understand the influences of kinds of fiber species, numbers of fiber metal laminated, thickness ratio between total coated figer metal laminated structure and thermal barrier as well as temperature distributed function on the values of thermal contact resistance between respective adjacent layers and temperature distribution from top to bottom surfaces for the coated figer metal laminated structure. Especially, the ratio of thermal contact resistance between maximum and minimum values are about five times no matter considering one or two kinds of fiber species. Besides the present results (mainly geometrical and physical parameters' effect) could guide engineers designing the coated figer metal laminated structures to adapt to high temperature environment especially aerospace temperature environment.

Key words: *coated figer metal laminated structure, separate variable method, equivalent temperature method, thermal contact resistance*

Introduction

It is well known that fiber metal laminated (FML) structure is a composite laminated structure consisting of some special fiber layer and metal layer, which integrates the excellent mechanical properties of both composite fiber and metal material [1, 2]. The FML structure is used widely in aerospace, internal combustion engines and other fields of the high temperature environment. However, the heat resistance capacity of the FML structure is limited at such extreme thermal environment. Therefore, it is necessary to consider a FML structure coated with an outer thermal barrier (CFML) and investigate the 3-D heat conduction problem for the CFML structure so as to avoiding the thermal damage for the inner FML structure.

For the composited structure coated with thermal barrier which subjected to high temperature environment, we have obtained analytical solutions of 3-D steady temperature field and 3-D steady thermodynamic analysis in previous work [3,4]. Bhowmick *et al.* [5] studied

---

friction and wear behavior of tetrahedral amorphous carbon and fluorinated ta-C coatings in the temperature range between 25 °C and 500 °C. Esposito *et al.* [6] gave optimization procedure and fabrication of highly efficient and thermally stable solar coating for receiver operating at high temperature. Based on infrared thermal wave testing technology, Liu *et al.* [7] studied thermal barrier coating debonding defects detection under linear frequency modulation heat excitation. However, most of previous researchers studied the behaviors of coating by means of experiments, the 3-D theoretical temperature model for the laminated structure coated with a thermal barrier under high temperature environment is reported hardly.

In addition the coating structure, the FML structure under thermal environment had aroused great interests among on researchers. The effect of thermal-shock cycles on the mechanical properties of FML structure had been evaluated by da Costa *et al.* [8]. Considering interfacial damage effect, Fu *et al.* [9, 10], Fu and Hu [11], and Li and Fu [12] investigated dynamic response and thermal postbuckling behavior of FML spherical/beam/plate under temperature field in detail. Tao *et al.* [13] concerned with the non-linear dynamic behaviors of FML beams subjected to moving loads in thermal environments. By utilizing fluent software, Qiu *et al.* [14] put forward a porous jump model to predict the breathability of laminated fabrics, and they studied the methods of determining the parameters for jump porous model so as to simplify the parameter setting process. However, the FML structure coated with an outer thermal barrier is mentioned rarely, especially the 3-D temperature model considering the thermal contact resistance for the CFML structure has not been reported for the moment.

On the present thermal contact resistance problem, by using harmonic mean value of thermal contact resistance, Seifert *et al.* [15] developed a transient comparative exponential method to measure the thermal conductivity of thin ceramic coatings. Huang and Xu [16] used the finite element method and regression method to explore the surface morphology effect on the thermal contact resistance and determine the temperature of the contact surface. Considering non-linear thermal boundary resistance, Tsai and Lee [17] analyzed the micro-scale heat transfer and ultrafast thermoelasticity in a multi-layered thin-film exposed to an ultra-short pulse laser. Patel and Gajjar [18] proposed an abrupt junction diode model to study the interface thermal resistance and thermal conductivity of composite. Zhao *et al.* [19] investigated effects of pressure and temperature on thermal contact resistance between different materials. A detailed heat pipe model was used by Sharifi *et al.* [20] to quantify the influence of the contact resistances on the heat transfer and fluid-flow within the heat pipe, as well as on the overall heat transfer rate. However, as far as we know, it is the first time using the novel equivalent-temperature method to solve 3-D thermal contact resistance problem and convective problem towards outside thermal environment for the CFML structure, which has not been found in previous papers.

The aim of this study is to give a novel equivalent-temperature model of 3-D steady heat conduction problem considering thermal contact resistance (between layers) and convective problem towards outside thermal environment for the CFML structure. In this study, the separate variable method (SVM) and equivalent temperature (ET) method are used comprehensively to solve the 3-D temperature field and value of thermal contact resistance between layers.

Mathematical modelling

Figure 1(a) is a CFML structure (composition of one outer thermal barrier and inner FML structure) under 3-D thermal environment, where the parameter symbols a and b represent length and width of the CFML structure, respectively, d_c and d are the thickness of the thermal barrier and FML layer, respectively, besides, $H = d + d_c$ is defined as total thickness of the CFML

structure. The Cartesian co-ordinate system *oxyz* is set on the mid-plane ($z = 0$) of the FML layer (the FML layer is assumed to be symmetrically laying about the mid-plane). Temperature distribution function $f(x, y)$ is applied on the top surface ($z = -d/2 - d_c$) of CFML structure, where the temperature increment $\Delta T = T - T_\infty$ on the other five surfaces except the top thermal barrier surface are zero (the five surfaces are assumed under adiabatic condition, *i. e.* the values of temperature increment at $x = 0$, a, $y = 0$, b, and $z = 0$ surfaces are zero), in which T and T_∞ are actual temperature and initial environmental temperature for the CFML structure, respectively. Figure 1(b) is the enlarged configuration of the CFML structure along z-co-ordinate, aluminum 2024-T3 is selected as representative metal material for the CFML structure, and S$_2$-glass fiber epoxy and glass-polymer are considered as two different fiber materials, respectively. Besides, the FML structure is laid symmetrically about x-axis, d_1, d_2,... d_5 are the respective thickness of layer from the top FML layer to the symmetrical surface (*i. e.* mid-plane of the FML structure).
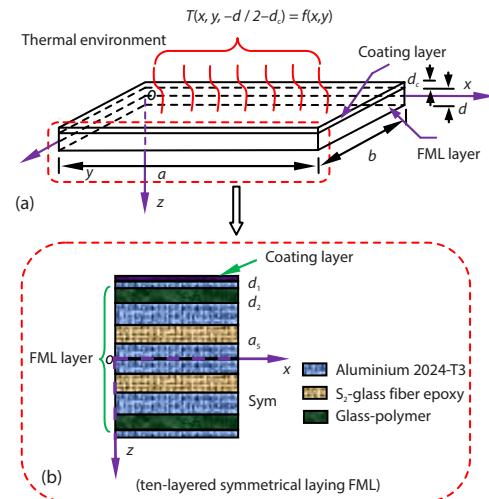

Figure 1. (a) Geometrical configuration of the CFML structure under 3-D thermal environment and (b) enlarged configuration of the CFML structure along z-co-ordinate

Heat conduction equation

Based on two following assumptions [21, 22]:
- Heat losses by radiation are negligible as compared to the intensity of the incident heat source.
- Thermal properties are considered constant and evaluated at an average temperature.

With the aforementioned assumptions, the 3-D steady-state heat conduction equation of the CFML structure that disregarding internal heat resource in the Cartesian co-ordinate is as [23]:

$$k_1 \frac{\partial^2 \Delta T}{\partial x^2} + k_2 \frac{\partial^2 \Delta T}{\partial y^2} + k_3 \frac{\partial^2 \Delta T}{\partial z^2} = 0 \tag{1}$$

where $0 < x < a$, $0 < y < b$, $-d/2 - d_c < z < d/2$, and k_i ($i = 1, 2, 3$) represent the thermal conductivities of the CFML structure along x-, y-, and z-directions, respectively.

According to fig. 1(a), the thermal boundary conditions of the CFML structure are considered:

$$\Delta T(0, y, z) = \Delta T(a, y, z) = 0 \tag{2a}$$

$$\Delta T(x, 0, z) = \Delta T(x, b, z) = 0 \tag{2b}$$

$$\Delta T\left(x, y, \frac{d}{2}\right) = 0 \tag{2c}$$

$$\Delta T(x, y, -d/2 - d_c) = f(x, y) \tag{2d}$$

1084

Gao, N., *et al.*: An Equivalent Temperature Model of 3-D Steady Heat ...
THERMAL SCIENCE: Year 2021, Vol. 25, No. 2A, pp. 1081-1094

Heat flux equation

Figure 2 represents a thermal network model for the CFML structure, there exists certain thermal contact resistance between thermal barrier and top of the FML layer as well as the thermal contact resistance between metal layer and composite layer for the FML structure (the thermal contact resistance only exists onc z-direction). In the fig. 2, red circle represents the starting point or ending point for the thermal barrier or respective metal and composite layer for the FML structure. Vertical dash line represents the abbreviated interlayer for the FML struc-
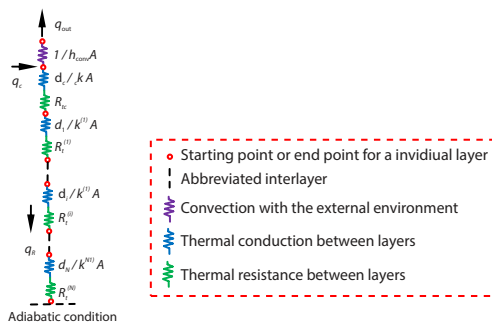

Figure 2. Thermal network model considering thermal resistance as shown in fig. 1(b)
(*for color image see journal web site*)

ture. Purple, blue, and green springs represent convection with external thermal environment, thermal conduction and thermal resistance effect between layers, respectively. The q_{out} on the top thermal barrier is the heat flux outflowing from the single thermal barrier to external thermal environment as other five surfaces are considered as adiabatic state (the values of temperature increment at $x = 0$, a, $y = 0$, b, and $z = 0$ surfaces are zero), q_R is the residual heat flux that based on heat conduction and thermal contact resistance, q_c the total heat flux flowing into the CFML structure:

$$q_{out} + q_R = q_c \tag{3}$$

where

$$q_{out} = \frac{T_\infty - T_c^-}{\left(\dfrac{1}{h_{conv} A}\right)}, \quad q_R = \frac{T_c^- - T_\infty}{\left(R_{tc} + \displaystyle\sum_{i=1}^{N-1} R_t^{(i)}\right) + \left(\dfrac{d_c}{k_c A} + \displaystyle\sum_{i=1}^{N-1} \dfrac{d_i}{k^{(i)} A}\right)} \tag{4}$$

where T_c^- is the actual temperature of upper surface for the thermal barrier, thus T_c^- equals to the $f(x, y) + T_\infty$ in present model. Similarly, in following text, the upper surface and bottom surface for arbitrary layer are instead of superscript symbol $^-$ and $^+$, respectively. The $1/h_{conv} A$ is the value of thermal convection between the top thermal barrier and external thermal environment, where h_{conv} and A are the convective heat transfer coefficient and cross-section area for the top thermal barrier, respectively, k_c – the heat conduction coefficient of the thermal barrier, R_{tc} – the thermal contact resistance between the thermal barrier and upper surface of the FML layer, d_i and $k^{(i)}$ are the thickness and heat conduction coefficient of the ith FML layer, respectively, $R_t^{(i)}$ – the thermal contact resistance between the $(i – 1)^{th}$ and i^{th} FML layer.

Solution methodology

In order to solve the temperature of bottom surface for the coated thermal barrier T_c^+, *i. e.* at $z = -(d/2)$ position, the equivalent temperature method is applied in fig. 3. From the figs. 3(a) and 3(b) are the geometrical configurations of the CFML structure and pure coating (*i. e.* thermal barrier) structure with the same thickness, respectively. Besides, the two models (CFML structure and pure coating) are subjected to the same thermal boundary conditions. Thus the temperature of bottom surface T_c^+ for the coating layer can be obtained when degenerating the CFML model, fig. 3(a), to the pure coating layer, fig. 3(b), of which the heat conduction equation for the pure coating layer can be re-written:

Gao, N., *et al.*: An Equivalent Temperature Model of 3-D Steady Heat ...
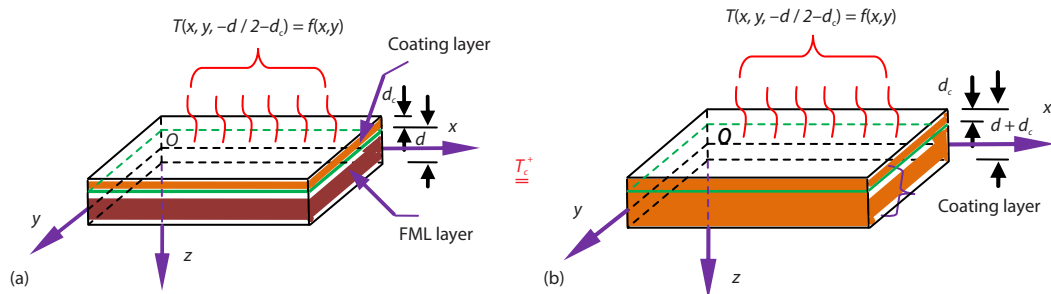THERMAL SCIENCE: Year 2021, Vol. 25, No. 2A, pp. 1081-1094

1085

Figure 3. Equivalent solution of the temperature at $z = -(d/2)$ position with the same heat boundary conditions; (a) geometrical configuration of CFML structure and (b) geometrical configuration of the coating structure

$$k_1^c \frac{\partial^2 \Delta T}{\partial x^2} + k_2^c \frac{\partial^2 \Delta T}{\partial y^2} + k_3^c \frac{\partial^2 \Delta T}{\partial z^2} = 0 \tag{5}$$

where k_i^c ($i = 1, 2, 3$) are thermal conductivities of pure coating layer along x-, y-, and z-directions, respectively. According to the fig. 3, the temperature of coating layer at $z = -(d/2)$ position for the CFML structure would not be changed when assuming the total thickness of coating layer is $d + d_c$. The SVM is applied to solve the 3-D steady temperature field, dispersing the temperature field as $\Delta T(x, y, z) = X(x)Y(y)Z(z)$ firstly, and substituting the separated variable form of temperature into eq. (5):

$$k_1^c X''(x)Y(y)Z(z) = -[k_2^c Y''(y)X(x)Z(z) + k_3^c Z''(z)X(x)Y(y)] \tag{6}$$

Dividing $X(x)Y(y)Z(z)$ on both sides of the eq. (6):

$$\frac{X''(x)}{X(x)} = -\left[\frac{k_2^c}{k_1^c}\frac{Y''(y)}{Y(y)} + \frac{k_3^c}{k_1^c}\frac{Z''(z)}{Z(z)}\right] \tag{7}$$

Herein defining following expression:

$$\frac{X''(x)}{X(x)} = -s^2 \tag{8}$$

Then, according to eqs. (7) and (8), the equation:

$$\frac{k_2^c}{k_1^c}\frac{Y''(y)}{Y(y)} + \frac{k_3^c}{k_1^c}\frac{Z''(z)}{Z(z)} = s^2$$

can be obtained.

From the previous eq. (2a), the following equations can be acquired:

$$X(0) = X(a) = 0 \tag{9}$$

Applying the eqs. (8) and (9), yields:

$$X_m(x) = G_m \sin sx \tag{10}$$

in which $s = m\pi/a$, $m = 1, 2, 3,...$, and defining following equation:

$$\frac{Y''(y)}{Y(y)} = \frac{s^2 k_1^c}{k_2^c} - \frac{k_3^c}{k_2^c}\frac{Z''(z)}{Z(z)} = -\mu^2 \tag{11}$$

Similar as the eq. (10), it can be obtained:

$$Y_n(y) = J_n \sin \mu x \tag{12}$$

where $\mu = n\pi/b$, $n = 1, 2, 3,...$, and defining

$$\omega_{mn}^2 = \frac{s^2 k_1^c + \mu^2 k_2^c}{k_3^c}$$

then with:

$$Z''(z) - \omega_{mn}^2 Z(z) = 0 \tag{13}$$

The general solution of unknown function $Z(z)$ can be solved:

$$Z_{mn}(z) = C_{mn} e^{\omega_{mn} z} + D_{mn} e^{-\omega_{mn} z} \tag{14}$$

According to eqs. (10), (12), and (14), the temperature increment ΔT is obtained:

$$\Delta T_{mn}(x, y, z) = G_m \sin \frac{m\pi x}{a} J_n \sin \frac{n\pi y}{b} (C_{mn} e^{\omega_{mn} z} + D_{mn} e^{-\omega_{mn} z}) \tag{15}$$

Simplifying previous eq. (15) based on eq. (2c):

$$\Delta T(x, y, z) = \sum_{n=1}^{\infty} \sum_{m=1}^{\infty} \Delta T_{mn}(x, y, z) =$$

$$= \sum_{n=1}^{\infty} \sum_{m=1}^{\infty} K_{mn} \sin \frac{m\pi x}{a} \sin \frac{n\pi y}{b} [e^{\omega_{mn} z} - e^{\omega_{mn}(d-z)}] \tag{16}$$

in which

$$D_{mn} = -C_{mn} e^{\omega_{mn} d}, \quad K_{mn} = G_m J_n C_{mn} \tag{17}$$

From the thermal boundary condition eq. (2d):

$$K_{mn} = \frac{4 \int_0^b \int_0^a f(x, y) \sin \frac{m\pi x}{a} \sin \frac{n\pi y}{b} \, \mathrm{d}x\mathrm{d}y}{ab \left[e^{-\omega_{mn}\left(\frac{d}{2} + d_c\right)} - e^{\omega_{mn}\left(\frac{3d}{2} + d_c\right)} \right]}, \quad (m = 1,3,5,...; n = 1,3,5,...) \tag{18}$$

According to eqs. (16) and (18), the temperature increment ΔT can be obtained:

$$\Delta T(x, y, z) = \sum_{n=1}^{\infty} \sum_{m=1}^{\infty} K_{mn} \sin \frac{m\pi x}{a} \sin \frac{n\pi y}{b} (e^{\omega_{mn} z} - e^{\omega_{mn}(d-z)}) \tag{19}$$

Then, the temperature increment of the coating layer at $z = -(d/2)$ position, ΔT_c^+, is obtained when substituting $z = -(d/2)$ into eq. (19):

$$\Delta T_c^+\left(x, y, -\frac{d}{2}\right) = \sum_{n=1}^{\infty} \sum_{m=1}^{\infty} K_{mn} \sin \frac{m\pi x}{a} \sin \frac{n\pi y}{b} \left(e^{-\frac{\omega_{mn} d}{2}} - e^{\frac{3\omega_{mn} d}{2}} \right) \tag{20}$$

Next, the temperature of bottom surface T_c^+ for the coating layer can be obtained immediately:

$$T_c^+ = \Delta T_c^+ + T_\infty \tag{21}$$

Gao, N., *et al.*: An Equivalent Temperature Model of 3-D Steady Heat ...
THERMAL SCIENCE: Year 2021, Vol. 25, No. 2A, pp. 1081-1094

1087

As each layer is of the same heat flux q_s for actual CFML heat transfer model:

$$\frac{T_{FML}^{1+} - T_c^{+}}{R_{tc} + \dfrac{d_1}{k^{(1)}A}} = \frac{T_{FML}^{2+} - T_{FML}^{1+}}{R_t^{(1)} + \dfrac{d_2}{k^{(2)}A}} = \cdots = \frac{T_{FML}^{(i+1)^+} - T_{FML}^{i^+}}{R_t^{(i)} + \dfrac{d_{i+1}}{k^{(i+1)}A}} = \cdots = \frac{T_{\infty} - T_{FML}^{(N-1)^+}}{R_t^{(N-1)} + \dfrac{d_N}{k^{(N)}A}} = q_s \tag{22}$$

According to the aforementioned eqs. (21) and (22), the values of thermal contact resistance and temperature for respective surfaces can be obtained finally.

Results and discussion

In the following examples, thermal barrier's heat conduction coefficient k_i^c and convection coefficient h_{conv} are in tab. 1. The composition of FML structure, aluminum 2024-T3, S$_2$-glass fiber epoxy and glass-polymer's thermal properties are listed in tab. 2 [9, 10].

Table 1. Principal temperature properties of thermal barrier

Heat conduction coeficient [Wm^{-1}K^{-1}]	Nature convection coefficient between air and coating layer [Wm^{-2}K^{-1}]
$k_1^c = 0.04$, $k_2^c = 0.04$, $k_3^c = 0.06$	$h_{conv} = 2$

Table 2. Principal temperature properties of aluminum 2024-T3, S$_2$-glass fiber epoxy and glass-polymer [9, 10]

Material	Heat conduction coefficient [Wm^{-1}K^{-1}]
Aluminum 2024-T3	$k_1 = 81.5$, $k_2 = 81.5$, $k_3 = 122.2$
S2-glass fiber epoxy	$k_1 = 0.33$, $k_2 = 0.33$, $k_3 = 0.5$
Glass-polymer	$k_1 = 0.13$, $k_2 = 0.13$, $k_3 = 0.19$

Example 1. In order to validate the presented theory and method in this paper, the problem is degenerated to a superalloy GH600 material and 3-D braid C/C composite material with thermal contact resistance effect. In the case, all geometrical and physical parameters as well as thermal property of superalloy GH600 material and braid C/C composite material are taken the same as Zheng *et al.* [24], such as cylindrical specimen's diameter and length are 300 mm and 400 mm, respectively. Besides the heat conduction coefficient of C/C composite material is assumed to be a constant value of 66.1 W/mK. Figure 4 was the thermal contact resistance test system for reference [24], the facility was based on Instron 8874 high temperature material testing machine and consists of a test column, a loading system, a heating and cooling unit and a temperature measurement system. Where the test column was composed of five components: a heat source, heat and force transfer bar, 14 thermal couples, 2 test specimens, and a heat sink. In present work, the thermal contact resistance of degenerated laminated structure can be also obtained based on aforementioned eqs. (21) and (22), and the comparison of variation of thermal contact re-
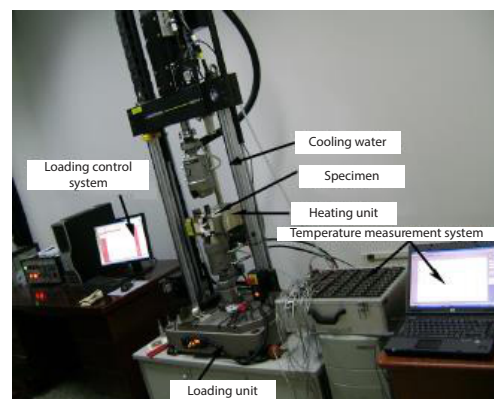

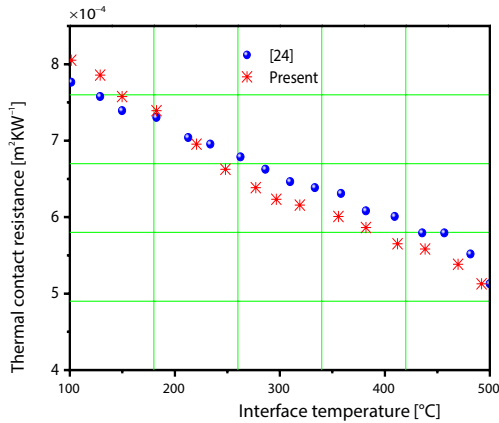**Figure 4. High temperature thermal contact resistance test system [24]**

1088

Gao, N., *et al.*: An Equivalent Temperature Model of 3-D Steady Heat ...
THERMAL SCIENCE: Year 2021, Vol. 25, No. 2A, pp. 1081-1094

Figure 5. Variation of thermal contact resistance with average interface temperature
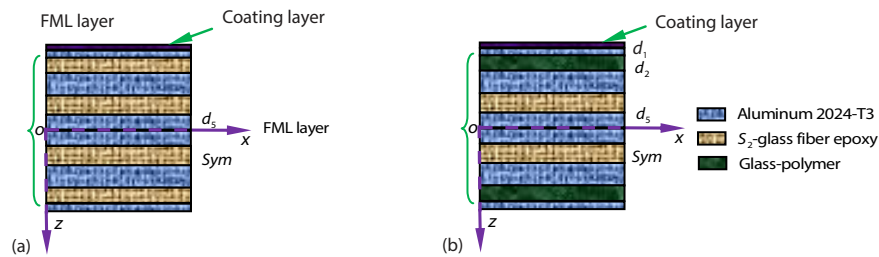

Figure 6. Geometrical configuration of two styles of CFML structure; (a) only S₂-glass fiber epoxy and (b) including S₂-glass fiber epoxy and glass-polymer (*for color image see journal web site*)

sistance with average interface temperature is seen in fig. 5, where the commercial software Wolfram MATHEMATICA 7.0 is applied in present computation. Without considering interface pressure, the result of Zheng *et al.* [24] (Instron 8874 facility is adopted in experimental investigation) is almost the same as such of present semi-analytical method, based on aforementioned eqs. (21) and (22), which shows feasibility of present theory and method.

Example 2. Figure 6(a) represents CFML structure only considering the S₂-glass fiber epoxy, fig. 6(b) the structure including the S₂-glass fiber epoxy as well as the glass-polymer, besides the two structures are of the same thickness for respective corresponding thermal bar-

rier, metal layer and composite layer. This example compares the values of thermal contact resistance and temperature from top to bottom surfaces along z co-ordinate. The major parameters in *Example 2*:

$$a = 1 \text{ m}, \quad b = 0.5 \text{ m}, \quad c = 0.004 \text{ m}, \quad 2(d_1 + d_2 + d_3 + d_4 + d_5) + d_c = 0.1 \text{ m}$$

$$d_1 : d_2 : d_3 : d_4 : d_5 = 1 : 3 : 5 : 4 : 3, \quad h_{\text{conv}} = 2 \text{ W/m}^2\text{K}, \quad f(x, y) = 100 \sin\frac{\pi x}{a} \sin\frac{\pi y}{b} \tag{23}$$

Figure 7 gives effect of kinds of fiber species on values of thermal contact resistance along non-dimensional co-ordinate Z^+. From fig. 7, the values of thermal contact resistance are almost the same at interfaces with the same constituent parts (at $z = 0$) for two different structures. The values of thermal contact resistance at the interfaces between thermal barrier and top FML layer reach maximum values for both two structures, while the minimum values are at the interfaces between two superimposed aluminum layers, the ratio of maximum and minimum value are about five times, which are consistent with actual situation. From the fig. 7, there only exists three different thermal contact resistances (coating-aluminum, aluminum-S₂-glass fiber epoxy, and aluminum-aluminum) for that only considering S₂-glass fiber epoxy structure, while there are four different thermal contact resistances (coating-aluminum, aluminum-glass-polymer, aluminum-S₂-glass fiber epoxy, and aluminum-aluminum) for that including S₂-glass fiber epoxy as well as glass-polymer. It can be concluded that adding ad-

Gao, N., *et al.*: An Equivalent Temperature Model of 3-D Steady Heat ...
THERMAL SCIENCE: Year 2021, Vol. 25, No. 2A, pp. 1081-1094

1089

ditional fiber would slow down the reduction rate of thermal contact resistance, which could be applied to the engineering practice directly. There is a little decrease for thermal contact resistance when adding additional glass-polymer at $z = 0$, $z = \pm d_5$, $z = \pm(d_4 - d_5)$, and $z = -(d_1 + d_2 + d_3 + d_4 + d_5)$, it can be attributed to the fact that heat conduction behavior has certain increase when adding additional glass-polymer material as the heat conduction coefficient of S_2-glass fiber epoxy is greater than that of glass-polymer material.

Figure 8 represents effect of kinds of fiber species on temperature values from top to bottom surfaces for the two different CFML structures along non-dimensional co-ordinate Z^*. From fig. 8, the temperature values at top and bottom surfaces are the same for this two different CFML structures. The maximum temperature value and minimum value at top surface and bottom surface are 393 K and 293 K, respectively. Besides, the temperature values at $z = 0$ and $z = -d_5$ (near $z = 0$) are merely the same. There exists an interesting thing that the temperature values that only considering S_2-glass fiber epoxy structure are less than that including S_2-glass fiber epoxy as well as glass-polymer structure at the $z > 0$ layers, but it does not occur at the $z < 0$ layers (*i. e.* curves do not display certain change rule). It can be inferred that the existence of coating layer affects the characteristic of symmetrical distribution for temperature variation.

Figure 7. Effect of number of fiber species on values of thermal contact resistance for the CFML structure along non-dimensional co-ordinate Z^+

Figure 8. Effect of number of fiber species on temperature values for the CFML structure along non-dimensional co-ordinate Z^+

Example 3. For the fig. 9(a) represents the six-layered laminated CFML structure, fig. 9(b) the ten-layered laminated CFML structure and fig. 9(c) the fourteen-layered laminated
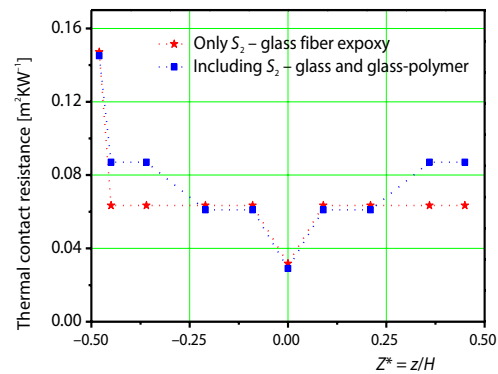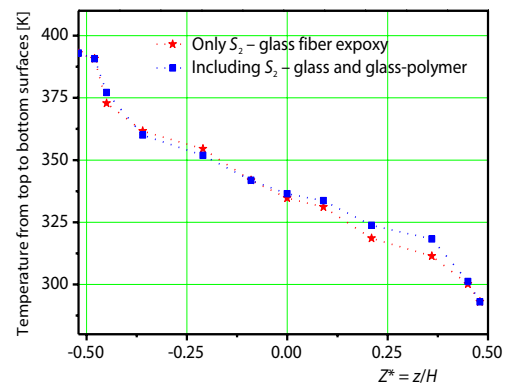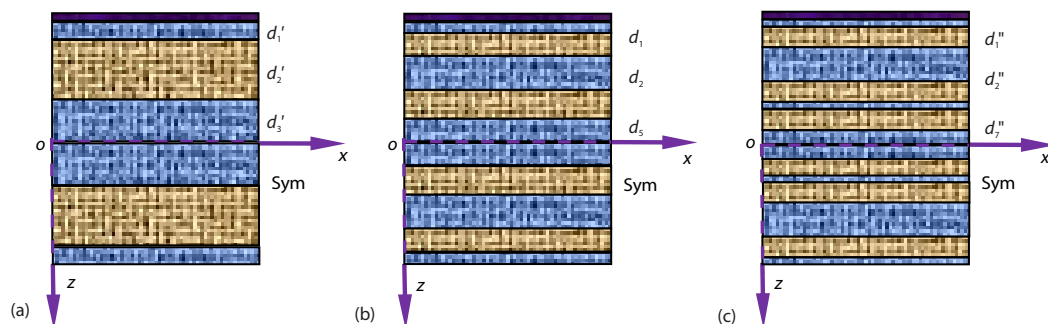

Figure 9. Geometrical configuration of CFML structures; (a) six-layered laminated CFML structure, (b) ten-layered laminated CFML structure, and (c) fourteen-layered laminated CFML structure (*for color image see journal web site*)

CFML structure. Besides, the three structures are of the same total thickness H. This example mainly compares the values of thermal contact resistance and temperature from top to bottom surfaces along z co-ordinate, and only S_2-glass fiber epoxy fiber are considered for three different structures.

The external geometrical parameters in this *Example 3*:

$$2(d_1' + d_2' + d_3') + d_c = 0.1\,\text{m}, \quad d_1' : d_2' : d_3' = 1 : 3 : 2$$

$$2(d_1 + d_2 + d_3 + d_4 + d_5) + d_c = 0.1\,\text{m}, \quad d_1 : d_2 : d_3 : d_4 : d_5 = 1 : 3 : 5 : 4 : 3$$

$$2(d_1'' + d_2'' + d_3'' + d_4'' + d_5'' + d_6'' + d_7'') + d_c = 0.1\,\text{m} \tag{24}$$

$$d_1'' : d_2'' : d_3'' : d_4'' : d_5'' : d_6'' : d_7'' = 1 : 3 : 5 : 3 : 1 : 3 : 2$$
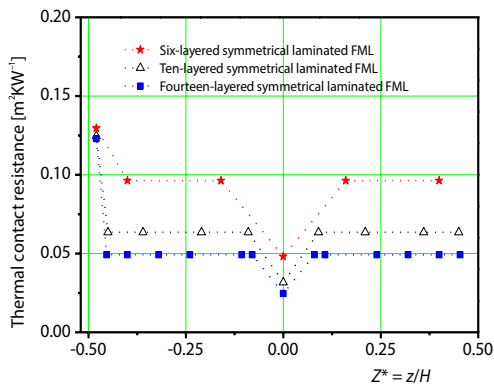

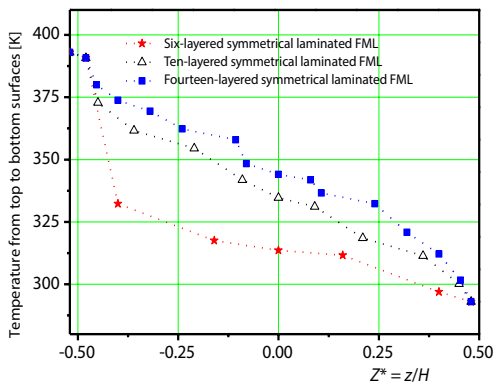Figure 10. Effect of number of FML layers on values of thermal contact resistance along non-dimensional co-ordinate Z^+

Figure 11. Effect of number of FML layers on temperature values from top to bottom surfaces along non-dimensional co-ordinate Z^*

Figure 10 shows effect of number of FML layers on values of thermal contact resistance for the CFML structure along non-dimensional co-ordinate Z^+. Figure 10, the value of thermal contact resistance decreases with the increasing of number of FML layers except at the interface between thermal barrier and top FML layer, besides the decrease amount tends to convergence gradually with the increasing of number of FML layers as the difference between ten-layer and fourteen-layer's values are far less than the difference between six-layer and ten-layer's values, the maximum values of thermal contact resistance at top surface are about 0.13 m^{2}K/W for three cases, while the minimum values of thermal contact resistance at mid-plane vary 0.025-0.05 m^{2}K/W. It can be obtained that total heat energy is dissipated by thermal contact resistance according to respective interface's thermal contact resistance ratio ontal amount of thermal contact resistance (considering three structures are of the same total heat flux flowing into structure).

Figure 11 indicates effect of number of FML layers on temperature values from top to bottom surfaces for the CFML structure along non-dimensional co-ordinate Z^*. From fig. 11, the temperature values increase with the increasing of number of FML layers at other locations (temperature values are the same onp and bottom surfaces), *i. e.* the temperature variation is more gentle with the increasing of number of FML layers. It can be attributed to the fact that the value of thermal contact resistance decreases with the increasing of number of FML layers, then the CFML structure retains greater temperature value.

Example 4. This example investigates effect of thickness ratio H/d_c on the values of thermal contact resistance and temperature from top to bottom surfaces along z co-ordinate for

Gao, N., *et al*.: An Equivalent Temperature Model of 3-D Steady Heat ...
THERMAL SCIENCE: Year 2021, Vol. 25, No. 2A, pp. 1081-1094

1091

ten-layered CFML structure which only considering S_2-glass fiber epoxy fiber. Only considering the change of thermal barrier's thickness, the basic geometrical and physical parameters of the CFML structure in this *Example 4*:

$$a = 1 \text{ m}, \ b = 0.5 \text{ m}, \ 2(d_1 + d_2 + d_3 + d_4 + d_5) + d_c = 0.1 \text{ m}, \ h_{\text{conv}} = 2 \text{ W/m}^2\text{K}$$

$$d_1 : d_2 : d_3 : d_4 : d_5 = 1 : 3 : 5 : 4 : 3, \ f(x,y) = 100 \sin\frac{\pi x}{a}\sin\frac{\pi y}{b} \tag{25}$$

Figure 12 gives effect of thickness ratio H/d_c on values of thermal contact resistance for the CFML structure along non-dimensional co-ordinate Z^*. From fig. 12, the maximum values of thermal contact resistance at top surface vary 0.16-0.045 m²K/W for three different thickness ratio H/d_c, while the minimum values of thermal contact resistance at mid-plane vary 0.035-0.01 m²K/W, *i. e.* the value of thermal contact resistance increases with the decreasing of coating thickness. It can be attributed to the fact that thermal barrier dissipates part of the heat energy, then residual heat energy are dissipated by interfaces' thermal contact resistance. Also, it can be concluded that the greater the thickness of thermal barrier is, the larger is the dissipating of heat energy by thermal contact resistance.

Figure 13 represents effect of thickness ratio H/d_c on values of temperature from top to bottom surfaces for the CFML structure along non-dimensional co-ordinate Z^*. From fig. 13, temperature values increase a little with the increasing of thickness ratio H/d_c at the same position except onp and bottom surfaces. It can be attributed to the fact that thick thermal barrier accelerates the decrease of temperature value. From the figs. 12 and 13, the conclusion that the effect of thickness ratio H/d_c on temperature value is far less than that on thermal contact resistance can be obtained immediately. And it can be ascribed to the parameter of energy's dissipation:

Figure 12. Effect of thickness ratio H/d_c on values of thermal contact resistance along non-dimensional co-ordinate Z^*
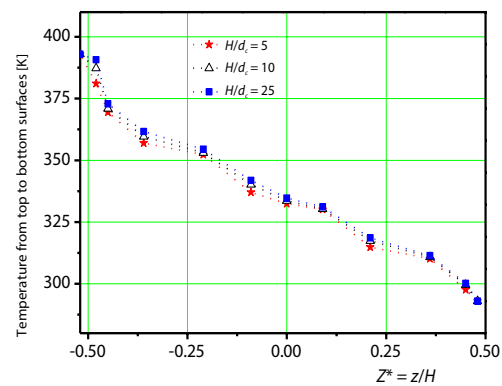
Figure 13. Effect of thickness ratio H/d_c on temperature values from top to bottom surfaces along non-dimensional co-ordinate Z^*

$$R_t^{(i)} = \frac{\Delta T}{q_n} \tag{26}$$

where q_n represents the heat flux normal to interface.

Example 5. This example mainly investigates effect of temperature distributed function $f(x, y)$ on the values of thermal contact resistance and temperature from top to bottom surfaces along z co-ordinate for ten-layered CFML structure that only considering S_2-glass fiber epoxy fiber. The major geometrical and physical parameters of the CFML structure in this *Example 5*:
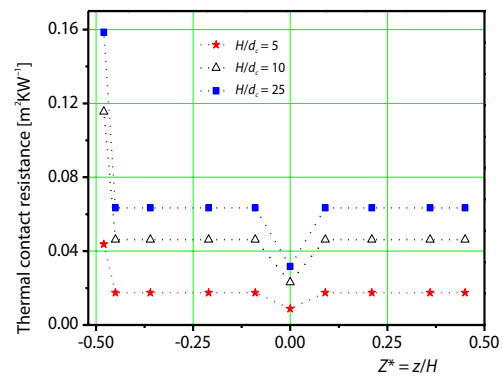
1092

Gao, N., *et al.*: An Equivalent Temperature Model of 3-D Steady Heat ...
THERMAL SCIENCE: Year 2021, Vol. 25, No. 2A, pp. 1081-1094

$$a = 1 \text{ m}, \ b = 0.5 \text{ m}, \ 2(d_1 + d_2 + d_3 + d_4 + d_5) + d_c = 0.1 \text{ m}$$

$$d_1 : d_2 : d_3 : d_4 : d_5 = 1 : 3 : 5 : 4 : 3, \ d_c = 0.004 \text{ m}, \ h_{\text{conv}} = 2 \text{ W/m}^2\text{K}$$
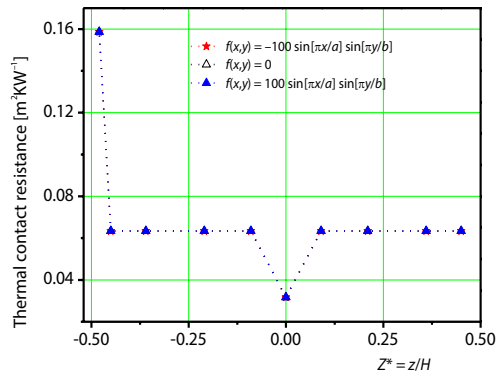
(27)

Figure 14. Effect of temperature distributed function *f(x, y)* on values of thermal contact resistance along non-dimensional co-ordinate *Z**
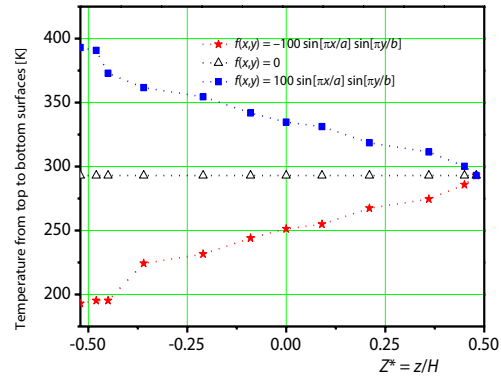
Figure 15. Effect of temperature distributed function *f(x, y)* on temperature values from top to bottom surfaces along non-dimensional co-ordinate *Z**

Figure 14 shows effect of temperature distributed function $f(x, y)$ on values of thermal contact resistance for the CFML structure along non-dimensional co-ordinate Z^*. From fig. 14, temperature distributed function $f(x, y)$ does not affect the value of thermal contact resistance for interfaces. It can be attributed to the fact that the thermal resistance is intrinsic behavior of structure and the change of temperature distributed function $f(x, y)$ would not affect any material behavior such as structure's mass and stiffness, hence not affect the value of thermal contact resistance finally.

Figure 15 indicates effect of temperature distributed function $f(x, y)$ on temperature values from top to bottom surfaces for the CFML structure along non-dimensional co-ordinate Z^*. From fig. 15, the temperature along Z^* co-ordinate is nearly a horizontal line basically when $f(x, y) = 0$ as there is no external heat flux flows into the CFML structure, and the temperature curves:

$$f(x, y) = \pm 100 \sin\left(\frac{\pi x}{a}\right) \sin\left(\frac{\pi y}{b}\right)$$

are symmetrical about the temperature curve for that of $f(x, y) = 0$. It can be seen clearly that the top surface of the CFML structure are under frozen and high temperature environment:

$$f(x, y) = -100 \sin\left(\frac{\pi x}{a}\right) \sin\left(\frac{\pi y}{b}\right) \ \text{and} \ f(x, y) = 100 \sin\left(\frac{\pi x}{a}\right) \sin\left(\frac{\pi y}{b}\right)$$

respectively. Besides the temperature for respective layer increases

$$f(x, y) = -100 \sin\left(\frac{\pi x}{a}\right) \sin\left(\frac{\pi y}{b}\right) \ \text{or decreases} \ f(x, y) = 100 \sin\left(\frac{\pi x}{a}\right) \sin\left(\frac{\pi y}{b}\right)$$

gradually from top to bottom surfaces and finally tends to environment temperature.

Conclusions

Based on balance principle of heat flux for each layer, an equivalent temperature model of the 3-D steady heat conduction analysis for a CFML structure is presented in present work. Thermal contact resistance between layers and temperature distribution from top to bottom

Gao, N., *et al.*: An Equivalent Temperature Model of 3-D Steady Heat ...
THERMAL SCIENCE: Year 2021, Vol. 25, No. 2A, pp. 1081-1094

1093

surfaces are investigated, as well as the effect of kinds of fiber species, number of FML layers, thickness ratio H/d_c and temperature distributed function $f(x, y)$. By means of numerical examples, some important conclusions can be drawn.

- Adding additional fiber would slow down the reduction rate of thermal contact resistance, the existence of thermal barrier affects the symmetrical-distribution characteristic of temperature variation for the CFML structure.
- Heat energy is dissipated by thermal contact resistance according to respective interface's thermal contact resistance ratio ontal amount of thermal contact resistance, the value of thermal contact resistance decreases with the increasing of number of the FML layers and then retains great temperature.
- The greater the thickness of thermal barrier is, the larger is the dissipating of heat energy by thermal contact resistance, besides thick thermal barrier accelerates the decrease of temperature value.
- Thermal contact resistance is intrinsic behavior of structure, change of temperature distributed function $f(x, y)$ would not affect any material behavior such as mass and stiffness, hence not affect the thermal contact resistance finally.

Conflict of interest

None declared.

Acknowledgment

Nomenclature

A – cross-section area for the top thermal barrier, [m²]

a, b – structure dimensions in x- and y-directions, [m]

d_c, d, H – thickness of thermal barrier, FML layer and total structure, [m]

d_i, d_i', d_i'' – thickness of ith layer for ten-layer, six-layer and fourteen-layer CFML structure, [m]

$f(x, y)$ – temperature distributed function, [K]

h_{conv} – coefficients of convective heat transfer, [Wm⁻²K⁻¹]

k_i – thermal conductivity coefficients of the CFML structure (i = 1, 2, 3), [Wm⁻¹K⁻¹]

$k^{(i)}$ – heat conduction coefficient of ith FML layers [Wm⁻¹K⁻¹]

k_i^c – heat conduction coefficients of the coating layer (i = 1, 2, 3), [Wm⁻¹K⁻¹]

m, n – number of Fourier series terms

q_c – total heat flux flowing into the CFML structure, [Wm⁻²]

q_{out} – heat flux outflow from single thermal barrier to external thermal environment, [Wm⁻²]

q_R – residual heat flux that resulted from heat conduction and thermal resistance effect, [Wm⁻²]

q_s – same heat flux flowing through interface, [Wm⁻²]

q_n – heat flux normal to interface, [Wm⁻²]

R_{tc} – thermal contact resistance between thermal barrier and upper surface of the FML layer, [m²KW⁻¹]

$R_i^{(i)}$ – thermal contact resistance between $(i-1)$th and ith FML layers, [m²KW⁻¹]

$\Delta T, T, T_\infty$ – temperature increment, actual temperature, and external surrounding environment, [K]

T_c^-, T_c^+ – acactual temperatures of upper surface and bottom surface for the thermal barrier, [K]

T_{FML}^{i+} – temperature of bottom surface for ith layer FML layer, [K]

Z^+ – non-dimensional quantities

References

[1]   Reyes, G. V., Cantwell, W. J., The Mechanical Properties of Fibre-Metal Laminates Based on Glass Fibre Reinforced Polypropylene, *Compos. Sci. Technol.*, *60* (2000), 7, pp. 1085-1094

[2]   Khalili, S. M. R., *et al.*, A Study of the Mechanical Properties of Steel/Aluminum/GRP Laminates, *Mat. Sci. Eng. A-Struct.*, *412* (2005), 1-2, pp. 137-140

[3]   Jiang, H. J., Dai, H. L., Analytical Solutions for 3-D Steady and Transient Heat Conduction Problems of a Double-Layer Plate with a Local Heat Source, *Int. J. Heat Mass Transfer*, *89* (2015), Oct., pp. 652-666

[4]   Jiang, H. J., *et al.*, 3-D Steady Thermodynamic Analysis for a Double-Layer Plate with a Local Heat Source and Harmonic Load, *Appl. Therm. Eng.*, *106* (2016), Aug., pp. 161-173

[5]   Bhowmick, S., *et al.*, High Temperature Tribological Behaviour of Tetrahedral Amorphous Carbon (ta-C) and Fluorinated ta-C Coatings Against Aluminum Alloys, *Surf. Coat. Tech.*, *284* (2015), Dec., pp. 14-25

[6]   Esposito, S., *et al.*, Optimization Procedure and Fabrication of Highly Efficient and Thermally Stable Solar Coating for Receiver Operating at High Temperature, *Sol. Energ. Mat. Sol. C.*, *157* (2016), Dec., pp. 429-437

[7]   Liu, Y. L., *et al.*, Thermal Barrier Coating Debonding Defects Detection Based on Infrared Thermal Wave Testing Technology under Linear Frequency Modulation Heat Excitation, *Thermal Science*, *23* (2019), 3A, pp. 1607-1613

[8]   Da Costa, A. A., *et al.*, The Effect of Thermal Cycles on the Mechanical Properties of Fiber-Metal Laminates, *Mater. Design*, *42* (2012), Dec., pp. 434-440

[9]   Fu, Y. M., *et al.*, Thermal Postbuckling Analysis of Fiber-Metal Laminated Plates Including Interfacial Damage, *Compos. Part B-Eng.*, *56* (2014), Jan., pp. 358-364

[10] Fu, Y. M., *et al.*, Analysis of Non-Linear Dynamic Response for Delaminated Fiber-Metal Laminated Beam under Unsteady Temperature Field, *Journal Sound Vib.*, *333* (2014), 22, pp. 5803-5816

[11] Fu, Y. M., Hu, S. M., Non-Linear Transient Response of Fibre Metal Laminated Shallow Spherical Shells with Interfacial Damage under Unsteady Temperature Fields, *Compos. Struct.*, *106* (2013), Dec., pp. 57-64

[12] Li, Y. L., Fu, Y. M., A Thermo-Elasto-Plastic Model for a Fiber-Metal Laminated Beam with Interfacial Damage, *Appl. Math. Model.*, *39* (2015), 12, pp. 3317-3330

[13] Tao, C., et al., Non-Linear Dynamic Analysis of Fiber Metal Laminated Beams Subjected to Moving Loads in Thermal Environment, *Compos. Struct.*, *140* (2016), Apr., pp. 410-416

[14] Qiu, L., *et al.*, Macro Fluid Analysis of Laminated Fabric Permeability, *Thermal Science*, *20* (2016), 3, pp. 835-838

[15] Seifert, S., *et al.*, Thermal Resistance and Apparent Thermal Conductivity of Thin Plasma-Sprayed Mullite Coatings, *Surf. Coat. Technol.*, *200* (2006), 11, pp. 3404-3410

[16] Huang, H .M., Xu, X. L., Effects of Surface Morphology on Thermal Contact Resistance, *Thermal Science*, *15* (2011), Suppl. 1, pp. S33-S38

[17] Tsai, T. W., Lee, Y. M., Analysis of Microscale Heat Transfer and Ultrafast Thermoelasticity in a Multi-Layered Metal Film with Non-Linear Thermal Boundary Resistance, *Int. J. Heat Mass Transfer*, *62* (2013), July, pp. 87-98

[18] Patel, P. P., Gajjar, P. N., Interface Thermal Resistance and Thermal Conductivity in Composites an Abrupt Junction Thermal Diode Model, *Phys. Lett. A*, *378* (2014), 34, pp. 2524-2528

[19] Zhao, Z., *et al.*, Effects of Pressure and Temperature on Thermal Contact Resistance between Different Materials, *Thermal Sci*ence, *19* (2015), 4, pp. 1369-1372

[20] Sharifi, N., *et al.*, The Influence of Thermal Contact Resistance on the Relative Performance of Heat Pipe-fin Array Systems, *Appl. Therm. Eng.*, *105* (2016), July, pp. 46-55

[21] Araya, G., Gutierrez, G., Analytical Solution for a Transient, 3-D Temperature Distribution Due to a Moving Laser Beam, *Int. J. Heat Mass Transfer*, *49* (2006), 21-22, pp. 4124-4131

[22] Jiang, H. J., Dai, H. L., Effect of Laser Processing on 3-D Thermodynamic Analysis for HSLA Rectangular Steel Plates, *Int. J. Heat Mass Transfer*, *82* (2015), Mar., pp. 98-108

[23] Jiang, H. J., *et al.*, Refined Plate Theory for Bending Analysis of a HSLA Steel Plate under 3-D Temperature Field, *Appl. Math. Comput.*, *250* (2015), Jan. pp. 497-51

[24] Zheng, X. P., *et al.*, Experimental Investigation of High Temperature Thermal Contact Resistance with Interface Material, *Theor. Appl. Mech. Lett.*, *1* (2011), 5, 051009